# Relaxor Ferroelectrics

Kenji UCHINO

*Department of Physics, Sophia University, 7-1, Kioi-cho, Chiyoda-ku, Tokyo 102, Japan*

# 緩和型強誘電体

内野研二

上智大学理工学部，102 東京都千代田区紀尾井町 7-1

緩和型強誘電性を構成イオンの無秩序配列性とからめて議論する．誘電性は温度依存性の小さい大誘電率と大きな周波数依存性（誘電緩和）で特徴付けられる．これらの性質は，微小な紡錘状分域の動的挙動によってうまく説明できる．電歪及び電気光学効果の優れた特性についても議論する．

[Received March 14, 1991]

**Ferroelectric relaxor characteristics are discussed in conjunction with the disordered arrangement of the constituent ions. Dielectric properties are characterized by giant and temperature-insensitive dielectric constants and large frequency dependence (dielectric relaxation). These properties are consistently explainable by the dynamic response of very small spindle-like domains. Superior characteristics in electrostriction and electrooptic effects are also discussed.**

***Key-words :*** *Relaxor ferroelectrics, Rattling ion model, Dielectric relaxation, Electrostriction, Diffuse phase transition, Disordered complex perovskite*

## 1. Introduction

AFTER Smolensky discovered that the ferroelectric phase transition of $Ba(Ti, Sn)O_3$ becomes diffused drastically with increasing the $BaSnO_3$ content,[1] phenomena of the diffuse phase transition have been investigated intensively. Figure 1 demonstrates the phase transition diffuseness in the permittivity curve in the $Ba(Ti, Sn)O_3$ system. At a temperature several tens ℃ above the permittivity peak, where the phase is supposed to be paraelectric and non-piezoelectric, the solid solution specimen was found to exhibit piezoelectric resonance.[2]

Other than these solid solution systems, very similar diffused phase transition can be observed in complex perovskite oxides such as $Pb(Mg_{1/3}Nb_{2/3})O_3$ and $Pb(Zn_{1/3}Nb_{2/3})O_3$, where two kinds of ions share B sites randomly.[3] Figure 2 shows the temperature dependence of the spontaneous polarization in $Pb(Zn_{1/3}Nb_{2/3})O_3$.[4),5] It is remarkable that the spontaneous polarization remains further above the permittivity-peak temperature (140℃). A similar trailing phenomenon is also observed in an electrooptic effect.[5] Temperature dependence of the permittivity of $Pb(Mg_{1/3}Nb_{2/3})O_3$ is plotted in Fig. 3, which obeys a special quadratic law[6),7]

$$1/\varepsilon \propto (T-T_0)^2, \qquad (1)$$

instead of the normal ferroelectric Curie-Weiss law

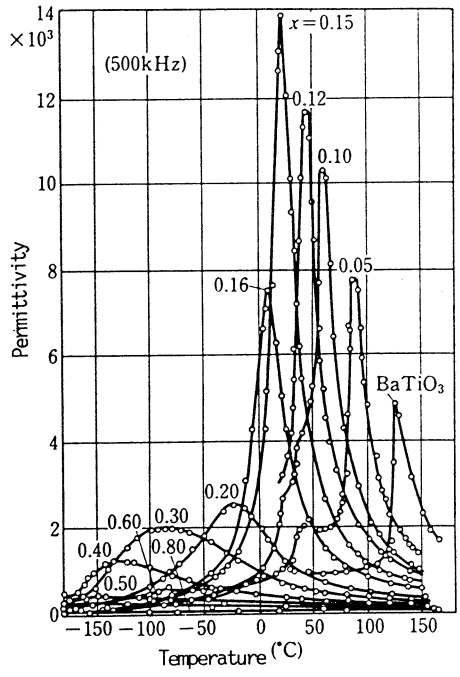


Fig. 1. Temperature dependence of permittivity in $(1-x)BaTiO_3$-$xBaSnO_3$.

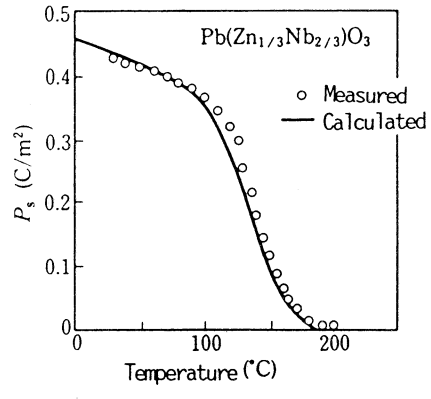


Fig. 2. Temperature dependence of the spontaneous polarization measured in a ⟨111⟩ single crystal of $Pb(Zn_{1/3}Nb_{2/3})O_3$.

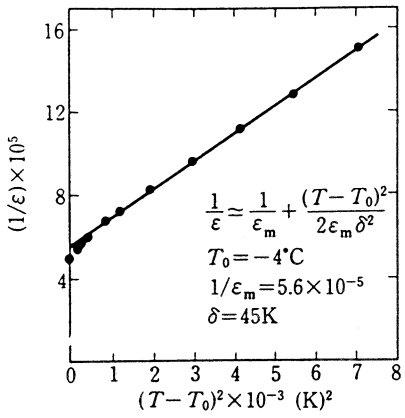


Fig. 3. Dependence of the reciprocal permittivity on the square of temperature measured in a $Pb(Mg_{1/3}Nb_{2/3})O_3$ single crystal.

$$1/\varepsilon \propto (T-T_0). \qquad (2)$$

## 2. Crystallographic structures of relaxor ferroelectrics

Relaxor ferroelectrics contain three categories of crystal structure; 1) solid solutions with a non-polar component ($BaTiO_3$–$BaSnO_3$), 2) atomic deficiencies by a dopant ($Pb^{2+}{}_{1-x}La^{3+}{}_x(Zr, Ti)_{1-x/4}V_{x/4}O_3$), and 3) complex perovskites with a combination of different valence ions ($A^{2+}(B^{2+}{}_{1/2}B^{6+}{}_{1/2})O_3$, $A^{2+}(B^{3+}{}_{1/2}B^{5+}{}_{1/2})O_3$, $A^{2+}(B^{2+}{}_{1/3}B^{5+}{}_{2/3})O_3$). It is worth to note that the amount of the atomic vacancy or the molar ratio of the B-site ions is definitely fixed so as to neutralize the valence charge.

Let us take some examples of complex perovskites; $Pb(Mg_{1/3}Nb_{2/3})O_3$, $Pb(Mg_{1/2}W_{1/2})O_3$, $Ba(Mg_{1/3}Ta_{2/3})O_3$. $Pb(Mg_{1/3}Nb_{2/3})O_3$ exhibits random arrangement of $Mg^{2+}$ and $Nb^{5+}$ ions on the B-site, and is called a disordered perovskite. On the contrary, $Pb(Mg_{1/2}W_{1/2})O_3$ shows an ordered arrangement of $Mg^{2+}$ and $W^{6+}$ in an NaCl-type as shown in Fig. 4(b) (1 : 1 order). The cation ordering is also found in $Ba(Mg_{1/3}Ta_{2/3})O_3$, where $Mg^{2+}$ and $Ta^{5+}$ are arranged in the sequence of $Mg^{2+}$–$Ta^{5+}$–$Ta^{5+}$ in the ⟨111⟩ direction (1 : 2 order, Fig. 4(c)).[8] The degree of the ionic ordering in complex perovskites depends basically on the difference in the valence charge or in the ionic radius.

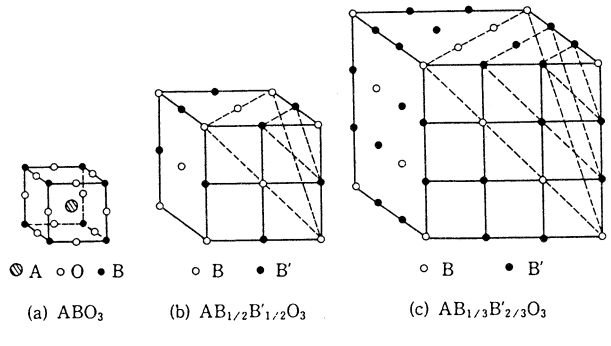


Fig. 4. Ordered arrangements of B-site ions in complex perovskites: (a) simple type, (b) 1 : 1 order type, (c) 1 : 2 order type.

The ordering of the ionic arrangement gives a significant effect to ferroelectricity. Simple perovskites exhibit either ferroelectricity ($BaTiO_3$, $PbTiO_3$) or antiferroelectricity ($PbZrO_3$, $PbHfO_3$). On the other hand, the 1 : 1 ordered complex perovskites tend to be antiferroelectric ($Pb(Mg_{1/2}W_{1/2})O_3$, $Pb(Co_{1/2}W_{1/2})O_3$), and disordered perovskites tend to be ferroelectric ($Pb(Mg_{1/3}Nb_{2/3})O_3$, $Pb(Fe_{1/2}Ta_{1/2})O_3$). In addition, the phase transition of the disordered perovskite is rather diffused and the crystal structure in the low temperature phase is to be rhombohedral.

The close relation between dielectric and crystallographic properties is suggestively exemplified in the previous work on $Pb(Sc_{1/2}Ta_{1/2})O_3$.[9] The degree of the cation ordering ($Sc^{3+}$, $Ta^{5+}$) is easily changeable only by thermal anneal without changing any composition. Figure 5 shows the differences in the dielectric constant (a) and the spontaneous polarization (b). The disordered sample exhibits a "diffuse" transition from a ferroelectric to a paraelectric phase. With increasing the ordering, the phase transition becomes "sharp" and occurs at a higher temperature. Moreover, the *P*–*E* curve at a temperature just below the transition shows a double hysteresis, indicating an antiferro-to-ferroelectric field-induced transition.

It is interesting to mention that the materials with the 1:2 cation order are usually non-polar and often applicable to microwave dielectrics.[10]

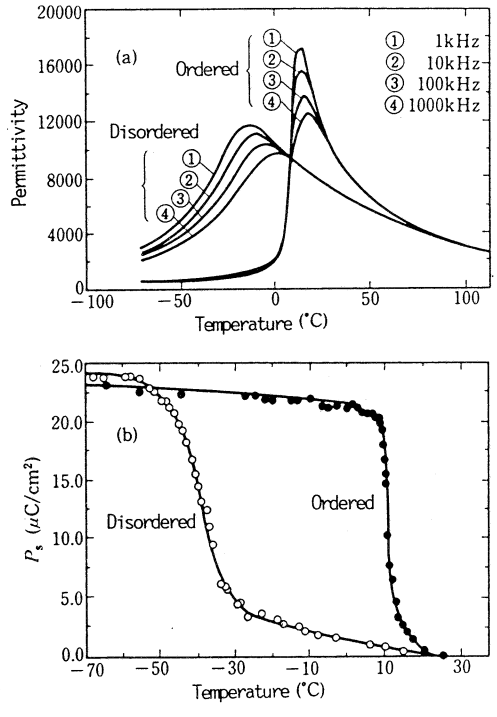


Fig. 5. Dielectric properties of single crystals of $Pb(Sc_{1/2}Ta_{1/2})O_3$ with cation-ordering ($S$=0.80) and without ordering ($S$=0.35): (a) permittivity and (b) spontaneous polarization.

## 3. Dielectric properties of relaxor ferroelectrics

The reasons why the relaxor ferroelectrics have been investigated intensively for capacitor applications are 1) their giant permittivity, and 2) temperature-insensitive characteristics (i.e. diffuse phase transition), in comparison with the normal perovskite solid solutions.

### 3.1 Origin of giant permittivity

An intuitive crystallographic model to explain the giant permittivity of the disordered perovskite has been proposed.[11] Figures 6(a) and 6 (b) show the ordered and disordered structures for an $A(B_{I\,1/2}B_{II\,1/2})O_3$ perovskite crystal. Assuming a rigid ion model, a large "rattling" space is expected for the smaller B ions in the disordered structure because the larger B ions prop open the lattice framework. Much less "rattling" space is expected in the ordered arrangement where neighboring atoms collapse systematically around the small B ions. The densely-packed structure of B ions in the ordered perovskite illustrated in Fig. 6(a) has been observed for $Pb(Mg_{1/2}W_{1/2})O_3$ based ceramics.[12]

When an electric field is applied to a disordered perovskite, the B ions with a large rattling space can shift easily without distorting the oxygen framework. Larger polarization can be expected for unit magnitude of electric field, in other words, larger dielectric constants and larger Curie-Weiss constants. On the other hand, in ordered perovskites with a very small rattling space, the B ions cannot move easily without distorting the octahedron. A smaller permittivity and a Curie-Weiss constant are expected.

### 3.2 Dielectric relaxation

Another significant characteristic of the "relaxor" ferroelectrics is dielectric relaxation (frequency dependence of permittivity) from which their name is originated. Temperature dependence of the permittivity in $Pb(Mg_{1/3}Nb_{2/3})O_3$ is plotted in Fig. 7 for various measuring frequencies. With increasing the measuring frequency, the permittivity in the low-temperature (ferroelectric) phase decreases and the peak temperature shifts towards the higher temperature; this is contrasted with the normal ferroelectrics such as $BaTiO_3$ where the peak temperature hardly changes with the frequency.

The dielectric relaxation similar in origin to the above-mentioned $Pb(Mg_{1/3}Nb_{2/3})O_3$ can be observed also in non-polar disordered perovskites. Figure 8(a) shows the permittivity–temperature curves of the $(K_{3/4}Bi_{1/4})(Zn_{1/6}Nb_{5/6})O_3$ single crystal.[13] The permittivity peak is not associated with the phase transition, and the cubic crystal structure is maintained through the measuring temperature. When we make a Cole–Cole plot of the real and imaginary parts of the permittivity (Fig. 8(b)), multi-dispersive characteristics can be observed especial-

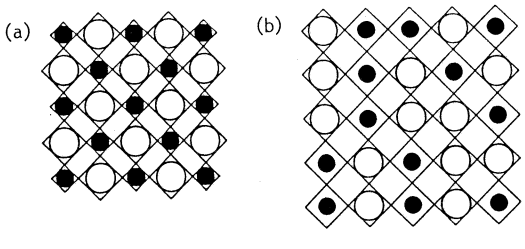


Fig. 6. Crystal structure models of the $A(B_{I1/2}B_{II\,1/2})O_3$ type perovskite: (a) ordered structure with a small rattling space and (b) disordered structure with a large rattling space (○=$B_I$ and ●=$B_{II}$).

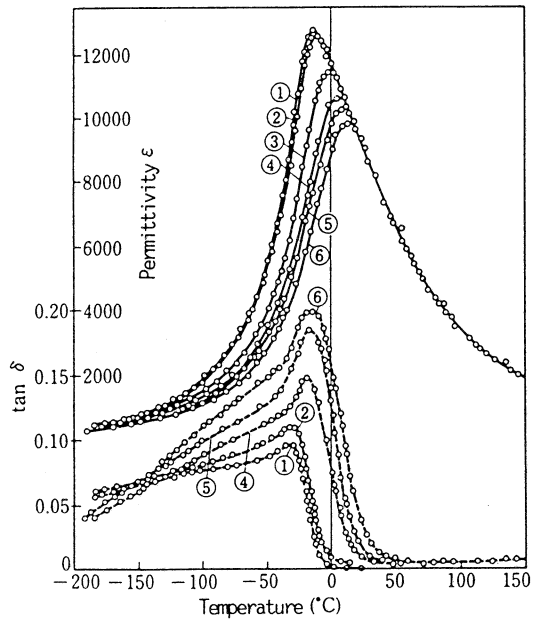


Fig. 7. Temperature dependence of the permittivity in $Pb(Mg_{1/3}Nb_{2/3})O_3$ for various measuring frequencies (kHz): (1) 0.4, (2) 1, (3) 45, (4) 450, (5) 1500, (6) 4500.

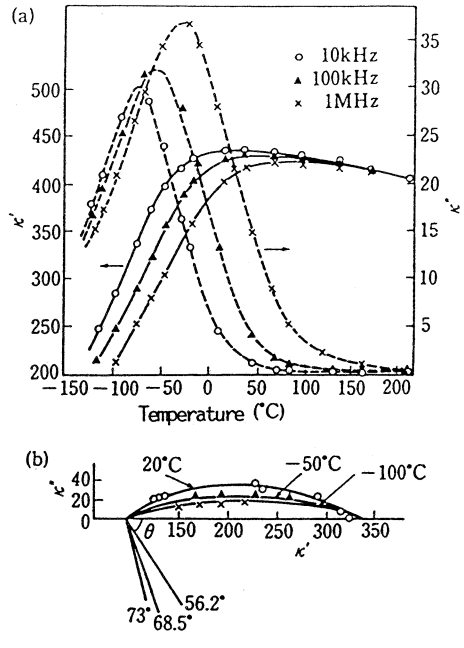


Fig. 8. (a) Permittivity vs. temperature curves of the $(K_{3/4}Bi_{1/4})(Zn_{1/6}Nb_{5/6})O_3$ single crystal. (b) Cole–Cole plot.

ly in a low temperature range. This is probably caused by shallow multi-potential-wells in a locally distorted perovskite cell due to the disordered ionic arrangement (Skanavi-type dielectric relaxation).[14] The ferroelectric relaxor may include a coupled phenomenon of a Skanavi-type relaxation and a ferroelectric phase transition (Fig. 9).

### 3.3 Analysis of the diffuse phase transition

The reason why the phase transition becomes diffused in the relaxor ferroelectrics is not clarified yet. We introduce here a "microscopic composition fluctuation" model which is most accepted.[15)-20)] Considering the Känzig region (the minimum size region in order to cause a cooperative phenomenon, ferroelectricity) in the range of 100–1000Å,[20)] the disordered perovskite such as $Pb(Mg_{1/3}Nb_{2/3})O_3$ reveals a local fluctuation of the distribution of $Mg^{2+}$ and $Nb^{5+}$ ions. Figure 10 shows a computer simulation of the composition fluctuation in the $A(B_{II1/2}B_{III1/2})O_3$-type crystal calculated for various degrees of the ionic ordering. The fluctuation of the $B_I/B_{II}$ fraction $x$ obeys a Gaussian error distribution.[19)] Krause reported the short-range ionic ordering of $Pb(Mg_{1/3}Nb_{2/3})O_3$ by electron microscopy.[21)] High resolution image in Fig. 11 reveals somewhat like ion-ordered islands in the range of 20–50Å.

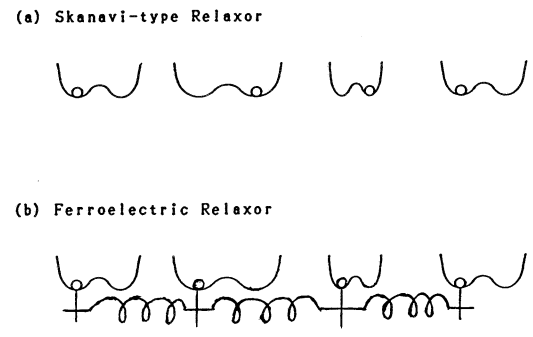


Fig. 9. Multi-potential-wells model for (a) Skanavi-type and (b) ferroelectric relaxors: Note the difference in the cooperative phenomenon.

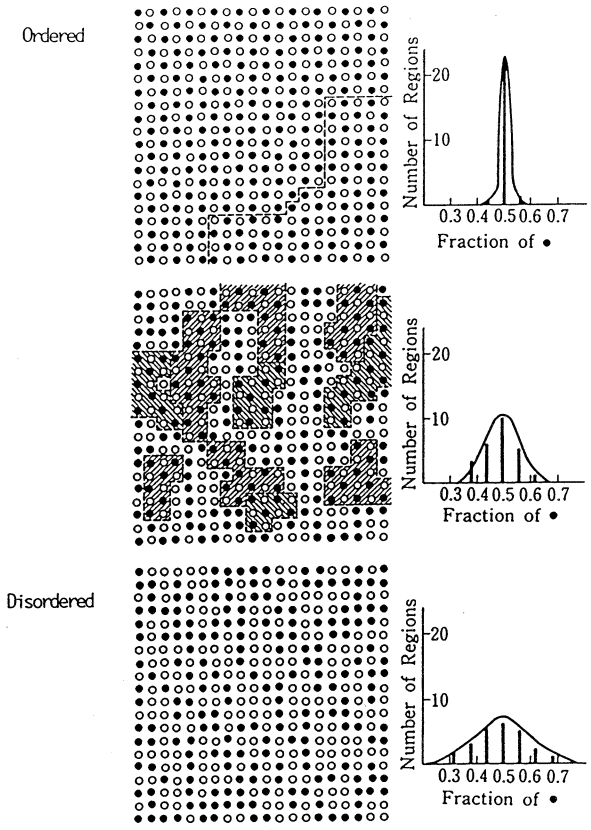


Fig. 10. Computer simulation of the composition fluctuation in the $A(B_{II1/2}B_{II1/2})O_3$ type calculated for various degrees of the ionic ordering (Känzig region size: $4\times4$).

According to Rolov et al., we assume that the physical properties in a local Känzig region may not change drastically due to the composition fluctuation, but that only the local Curie temperature $\theta$ should be changed in proportion to the fluctuation $\Delta x(=x-x_{av})$, i.e.

$$r=(\theta-\theta_{av})/(x-x_{av}), \tag{3}$$

where $\theta_{av}$ is an average Curie temperature and $r$ is a constant. Then the distribution of the local Curie temperature is given by

$$f(\theta)=(1/\sqrt{2\pi\sigma^2})\exp[-(\theta-\theta_{av})^2/2\sigma^2], \tag{4}$$

where $\sigma$ is the standard deviation.

Based on this statistical distribution of the Curie temperature and the ferroelectric phenomenology, physical properties can be estimated theoretically. If the fluctuation of the local composition (not a semi-macroscopic compositional inhomogeneity!) is large enough to provide $\sigma\gg10$°C, the normal Curie-Weiss law

$$1/\varepsilon=(T-T_0)/C \quad (T_0\text{: Curie-Weiss temperature}) \tag{5}$$

is transformed into

$$1/\varepsilon=(1/\varepsilon_m)\exp[-(T-\theta_{av})^2/2\sigma^2]=(1/\varepsilon_m)[1+(T-\theta_{av})^2/2\sigma^2+(T-\theta_{av})^4/8\sigma^4+\cdots], \tag{6}$$

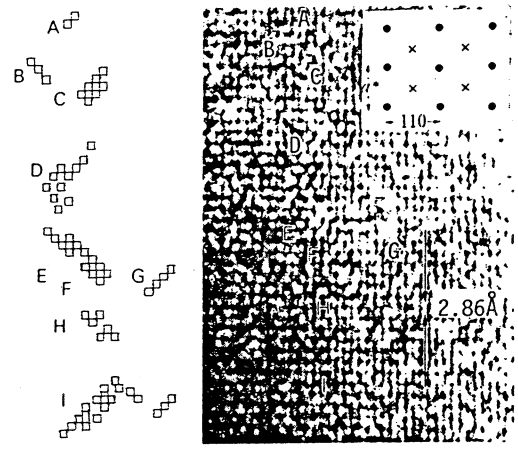


Fig. 11. High resolution electron-microscopic image of the $Pb(Mg_{1/3}Nb_{2/3})O_3$ single crystal ((110) plane). Note ion-ordered islands in the range of 20–50Å.

where $\varepsilon_m$ is the maximum permittivity at $T=\theta_{av}$. Equation (6) corresponds reasonably to an experimental result of Eq. (1) in the diffuse phase transition.

### 3.4 Domains in relaxor ferroelectrics

Let us review the recent studies on the dynamic domain observation in relaxor ferroelectrics.[22] Figure 12 shows some examples of the ferroelectric domains observed in the solid solution system $(1-x)Pb(Zn_{1/3}Nb_{2/3})O_3$–$xPbTiO_3$. The system exhibits a drastic change from a diffuse phase transition to a sharp transition with an increase of the $PbTiO_3$ content $x$, correlating to the existence of a morphotropic phase boundary from a rhombohedral to a tetragonal phase around $x=0.1$ as shown in Fig. 13.

Very small spindle-like domains ($\sim 5\ \mu m$) with ambiguous boundaries in $x=0$ become larger and clearer with increasing $x$. It is noteworthy that the specimen of $x=0.095$ reveals a two-stage domain structure, i.e. spindle-like domains included in clear straight boundaries; this is probably due to the coexistence of the rhombohedral and tetragonal phases at room temperature.

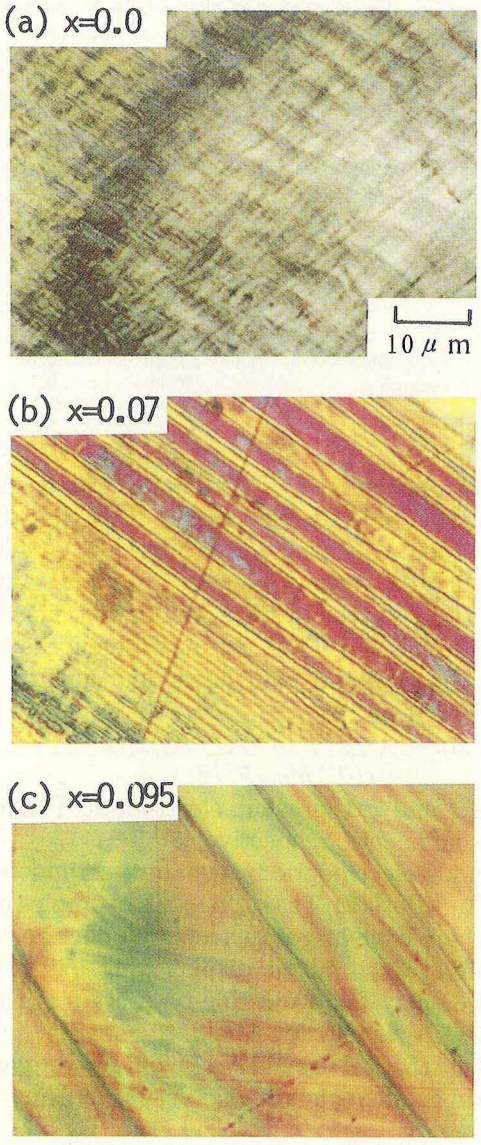


Fig. 12. Ferroelectric domains in the $(1-x)Pb(Zn_{1/3}Nb_{2/3})O_3$–$xPbTiO_3$ system: Note the ambiguous small spindle-like domains in relaxor ferroelectrics.

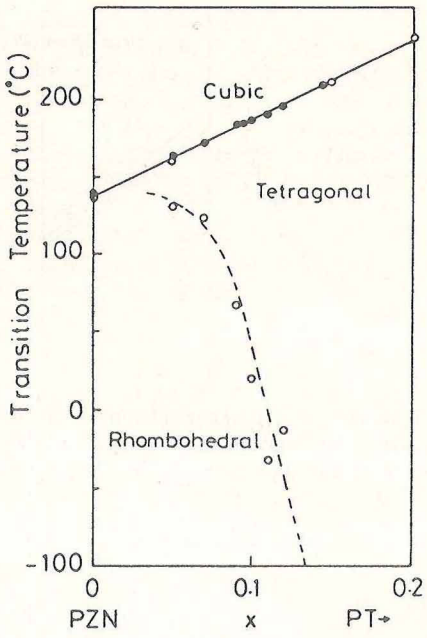


Fig. 13. Phase diagram of the $(1-x)Pb(Zn_{1/3}Nb_{2/3})O_3$–$x\ PbTiO_3$ system.

Dynamic response to an electric field gives also important information. The ambiguous domain boundaries in $x=0$ move slowly changing their shape, while the clear straight boundaries in $x=0.095$ move rather quickly keeping the original shape. This probaly explains the dielectric relaxation in the room temperature phase in lead zinc niobate.

## 4. Electrostriction in relaxor ferroelectrics

Since the cation-disordered complex perovskite exhibits a diffuse phase transition, the crystal is electrically-poled easily when an electric field is applied around the transition temperature, and depoled completely without any remanent polarization because the domain is separated into micro-domains when the field is removed. This provides rather large apparent secondary effects in physical properties.

Concerning electric-field induced strains, $Pb(Mg_{1/3}Nb_{2/3})O_3$ for example, exhibits a large electrostriction (i.e. a second-order electromechanical property where strain is induced in proportion to the square of the applied field) at room temperature in the small electric-field range. Figure 14 shows the strain curve of the transversely induced electrostriction in $0.9Pb(Mg_{1/3}Nb_{2/3})O_3$–$0.1PbTiO_3$.[23)-26)] The relaxor ceramics are anhysteretic, and retrace the same curve with rising and falling fields. For comparison, the piezoelectric strain (i.e. strain induced in proportion to the applied field) of a hard PZT 8 under cyclic field is also plotted in Fig. 14. This material has often been used in the fabrication of multi-

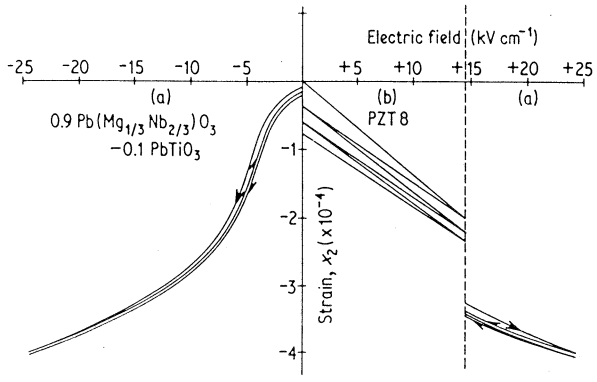


Fig. 14. Transverse strain in ceramic specimens of (a) 0.9 Pb $(Mg_{1/3}Nb_{2/3})O_3$–0.1$PbTiO_3$ and (b) a typical hard PZT8 piezoceramic under slowly varying electric fields.

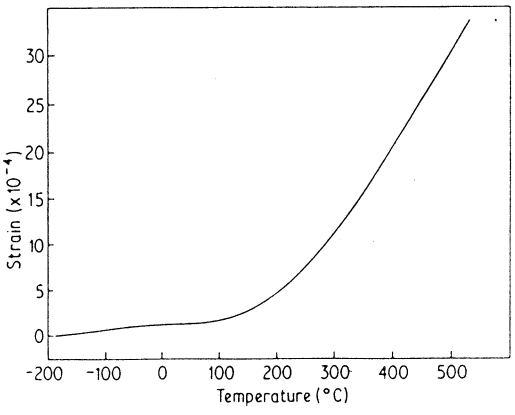


Fig. 15. Thermal expansion in polycrystalline 0.9Pb$(Mg_{1/3}Nb_{2/3})O_3$–0.1$PbTiO_3$.

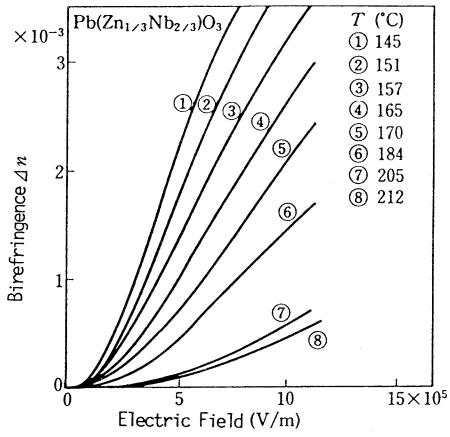


Fig. 16. Birefringence vs. electric field relation of $Pb(Zn_{1/3}Nb_{2/3})O_3$ in the paraelectric phase.

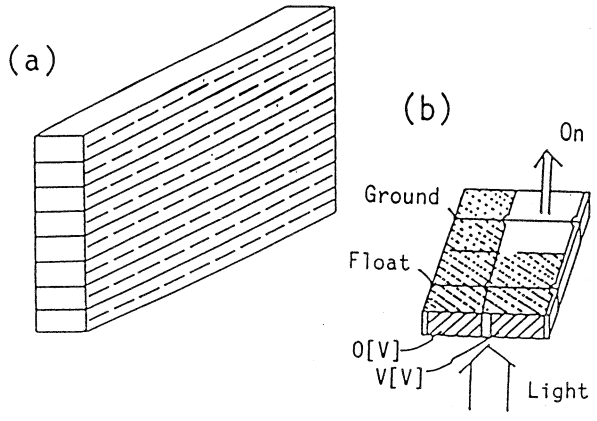


Fig. 17. Two-dimensional display for projection-type TV's using PLZT ceramics.

dither mirrors and other active optical components. Note that the electrostriction is comparable to or larger than the magnitude of the typical piezoelectric strain induced in $Pb(Zr, Ti)O_3$ based ceramics and far more reproducible under cyclic drive conditions.

Another interesting property of relaxor ferroelectrics is the very small thermal expansion effect throughout the Curie range. Figure 15 shows the thermal strain of 0.9$Pb(Mg_{1/3}Nb_{2/3})O_3$–0.1$PbTiO_3$ plotted as a function of temperature.[23] In the temperature range $-100°$ to $+100°C$, the thermal expansion coefficient is less than $1\times10^{-6}\ K^{-1}$, comparable to the best low-expansion ceramics or fused silica. The thermal strains are far smaller than the electrostrictive strains, which is extremely advantageous for micropositioner applications.

## 5. Electrooptic effect

Relaxor ferroelectrics are also remarked in nonlinear optic applications because an extraordinarily large electrooptic Kerr effect can be observed even in the so-called paraelectric state. Figure 16 shows the birefringence versus electric field relation of $Pb(Zn_{1/3}Nb_{2/3})O_3$ in the paraelectric phase.[5] The parabolic curve in the low field region tends to approach a straight line in the high field region. This peculiar phenomenon is analyzed on the basis of the model that the crystal is composed of the ferroelectric and paraelectric phases mixed together. Suppose that the volume fraction of the paraelectric phase $x(T)$ is given by the accumulated Gaussian distribution (See Eq. (4)), the birefringence is estimated by the summation of linear and quadratic electrooptic effects:[18]

$$\Delta n=[1-x(T)n^3(r_{33}-r_{13})E/2 +x(T)n^3g_{44}P^2/2, \qquad (7)$$

where $r$ and $g$ represent electrooptic Pockels and Kerr coefficients, respectively.

Famous electrooptic transparent ceramics PLZT, i.e. $(Pb_{1-x}La_x)(Zr_yTi_z)_{1-x/4}O_3$, are examples of relaxors, which have large electrooptic effect and are applicable to light valves, displays, etc. A two-dimensional display for projection-type TV's is shown in Fig. 17.[27] Newly developed transparent ceramics $(1-x)Pb(Mg_{1/3}Nb_{2/3})O_3-xPbTiO_3$ with giant electrooptic coefficients are also very promising materials.

## 6. Summary

Ferroelectric relaxor characteristics are closely

related with the disordered arrangement of the constituent ions. Dielectric properties are characterized by giant and temperature-insensitive dielectric constants and large frequency dependence (dielectric relaxation). These properties are consistently explainable by the dynamic response of very small spindle-like domains. Superior characteristics in electrostriction and electrooptic effects are also attributed to the easy poling of the ferroelectric micro-domains.

## References


1) G. A. Smolensky, *J. Phys. Soc. Jpn.*, 28, Suppl., 26 (1970).
2) G. A. Smolensky and V. A. Isupov, *Zh. tech. Fiz.*, 24, 1375 (1954).
3) G. A. Smolensky, V. A. Isupov, A. I. Agranovskaya and S. N. Popov, *Sov. Phys.-Solid State*, 2, 2584 (1961).
4) S. Nomura, M. Abe, F. Kojima and K. Uchino, *Jpn. J. Appl. Phys.*, 14, 1881 (1975).
5) F. Kojima, J. Kuwata and S. Nomura, Proc. 1st Meeting on Ferroelectric Mater. & Appl. (Kyoto, 1977) p. 155.
6) V. V. Kirillov and V. A. Isupov, *Ferroelectrics*, 5, 3 (1973).
7) K. Uchino, S. Nomura, L.E. Cross, S. J. Jang and R. E. Newnham, *J. Appl. Phys.*, 51, 1142 (1980).
8) G. Blasse and A. F. Corsmit, *J. Sol. State Chem.*, 6, 513 (1973).
9) N. Setter and L. E. Cross, *J. Appl. Phys.*, 51, 4356 (1980).
10) S. Nomura, K. Toyama and K. Kaneta, *Jpn. J. Appl. Phys.*, 21, L624 (1982).
11) K. Uchino, L. E. Cross, R. E. Newnham and S. Nomura, *J. Phase Transitions*, 1, 333 (1980).
12) A. Amin, R. E. Newnham, L. E. Cross, S. Nomura and D. E. Cox, *J. Sol. State Chem.*, 35, 267–71 (1980).
13) S. Nomura and F. Kojima, *Jpn. J. Appl. Phys.*, 12, 205 (1973).
14) G. I. Skanavi, I. M. Ksendzov, V. A. Trigubenko and V. G. Prokhvatilov, *Soviet Phys.-JETP*, 6, 250 (1958).
15) V. A. Isupov, *Zh. tech. Fiz.*, 26, 1912 (1956).
16) B. N. Rolov, *Fiz. Tverdogo Tela*, 6, 2128 (1963).
17) V. A. Isupov, *Izv. Akad. Nauk SSSR*, Ser. Fiz., 28, 653 (1964).
18) J. Kuwata, K. Uchino and S. Nomura, *Ferroelectrics*, 22, 863 (1979).
19) K. Uchino, J. Kuwata, S. Nomura, L. E. Cross and R. E. Newnham, *Jpn. J. Appl. Phys.*, 20, Suppl. 4, 171 (1981).
20) W. Känzig, *Helv. Phys. Acta*, 24, 175 (1951).
21) H. B. Krause, J. M. Cowley and J. Wheatley, *Acta Cryst.*, A35, 1015 (1979).
22) K. Kato, K. Suzuki and K. Uchino, *Seramikkusu Ronbunshi* (*J. Ceram. Soc. Japan*), 98, 840–45 (1990).
23) L. E. Cross, S. J. Jang, R. E. Newnham, S. Nomura and K. Uchino, *Ferroelectrics*, 23, 187 (1980).
24) K. Uchino, S. Nomura, L. E. Cross, R. E. Newnham and S. J. Jang, *J. Mater. Sci.*, 16, 569 (1981).
25) K. Uchino, "Piezoelectric/Electrostrictive Actuators", Morikita Pub. Co., Tokyo (1986).
26) K. Uchino, "Ceramic Actuators", Fine Ceramics Soc. Bull., Internation. Ed. (1988) p.23.
27) K. Ohmura, Y. Murai, K. Uchino and J. Giniwitcz, Proc. International Display Research Conf., IEEE (1988) p. 137.


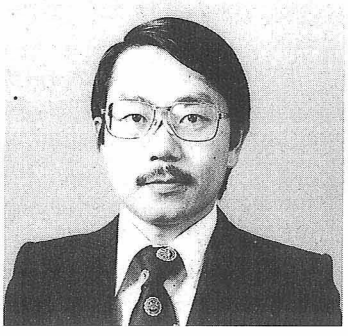


Kenji UCHINO is presently an Associate Professor, Faculty of Science and Technology, Sophia University. His professional field is applied solid state physics (ferroelectrics).

*Education*: Master of Engineering in Physical Electronics, Tokyo Institute of Technology, Tokyo, Japan, 1975; Doctor of Science in Physical Electronics, Tokyo Institute of Technology, Tokyo, Japan, 1981.

*Previous Occupations*: Research Associate of Tokyo Institute of Technology, 1976; Research Associate of Materials Research Laboratory, The Pennsylvania State University, 1978; Associate Professor of Sophia University, 1985; Visiting Professor of The Pennsylvania State University, 1991.

*Professional Activities*: Member of Physical Society of Japan, Japanese Society of Applied Physics, Ceramic Society of Japan, American Ceramic Society, and IEEE; Chairman of Society of Solid State Actuators, JITAS, MITI.

*Awards*: Best Paper Award in Japanese Society of Oil/Air Pressure Control; Best Movie Memorial Award in Japan Scientific Movie Festival, Academic Award in Nissan Motors Scientific Foundation, March 1990.